

Electric Field Distributions in Dielectrics, with Special Emphasis on Near-Surface Regions in Ferroelectrics

Philip E. Bloomfield

*Department of Physics, The City College of the City University of New York,
New York, New York 10031*

and

I. Lefkowitz and A. D. Aronoff

Pitman-Dunn Research Laboratories, Frankford Arsenal, Philadelphia, Pennsylvania 19137

(Received 16 February 1971)

The characteristics of the electric field distribution due to space-charge currents in dielectric materials with both linear and nonlinear polarization are discussed, and analytic and numerical solutions for zero current are presented. In considering Poisson's equation for a material with a position-dependent polarization, we find it convenient to define a dielectric parameter in terms of the internal-electric-field derivative of the polarization rather than their quotient. In the static situation the largest electric fields exist near the surfaces for all dielectrics. Introducing the nonlinear dielectric parameter into the one-carrier model including diffusion exaggerates the effect. We expect that the strongest indications for such behavior occur in ferroelectrics since their dielectric properties are the most field sensitive. The diffusionless two-carrier recombination-center model is briefly considered. We discuss an example from the literature in terms of our "amplified-space-charge region" model and comment upon implications for device usage.

I. INTRODUCTION

Since 1955¹ numerous investigators using many different techniques have found that a surface layer exists in ferroelectric BaTiO₃ crystals. These experiments are discussed in recent reviews and monographs.²⁻⁵ The observed effects and experiments are not directly interrelated, and several different models have been introduced to explain the experimental results of different investigators. The majority of these models for the surface layers fall into two classes. Many of these experiments discussed in the reviews have led to models which contain *high field gradients* near the surface.⁶⁻¹¹ Other recent experiments not referenced in the reviews²⁻⁵ are consistent with this view (first proposed by Känzig¹) that surface anomalies are due to the existence of a surface layer of high electric field (10⁶ V/cm) of thickness 10⁻⁴-10⁻⁶ cm. The experiments include the anomalous radiation sensitivity of BaTiO₃ reported by Lefkowitz and co-workers,¹²⁻¹⁴ and Van Lint and Wyatt,¹⁵ and the electron-mirror microscopy experiments by English^{16,17} which give a direct view of the surface-potential distribution.

Other experiments are explainable in terms of models which have a layer of *low-dielectric-constant* material at the surface.¹⁸⁻²¹ Merz³ has pointed out that the dielectric constant in ferroelectrics is highly nonlinear and field dependent; thus, it would be possible for the dielectric constant to vary within the material.

We wish to show that these two classes of models

are consistent with one another. The polarization curves in a perovskite ferroelectric indicate that large applied potential differences cause a decrease in the dielectric constant; furthermore, Poisson's equation implies that a dielectric constant which is field dependent can have a profound effect on the magnitude of the internal electric field.

It is well known that applying a potential difference to a dielectric can lead to the formation of space-charge regions and very large electric fields near the surface of an insulating crystal.²²⁻²⁵ These fields are a very sensitive function of the space-charge density and distribution. For nonlinear dielectrics quite anomalous surface effects can be expected which are actually not due to anomalous properties of the surface per se, but can be attributed to the space-charge fields and the behavior of the *bulk* dielectric constant in regions of high electric field. Particularly dramatic effects are expected in strongly nonlinear dielectrics such as ferroelectrics, where the space-charge field at the surface can be strong enough to "saturate" the dielectric near the surface. Under these circumstances, the dielectric constant K at the surface may vary from extremely large values in regions of small internal electric field to values ($\approx 5-10$) reduced by several orders of magnitude in larger internal-field regions. At the same time, the decrease of the dielectric constant causes this electric field to further increase to very high values. It should be noted that for some materials such as BaTiO₃,⁷ large changes in polarization are concomitant with structural phase changes so that the

layered electric field structures we describe may imply layers of different crystalline phase.

In the following we discuss the interdependence of the dielectric constant and the electric field in those insulating materials in which the electric field is strongly position dependent and the dielectric constant is field dependent.

II. THEORY OF MUTUAL INFLUENCE OF VARIABLE DIELECTRIC CONSTANT AND INTERNAL-ELECTRIC-FIELD DISTRIBUTION

We now develop and describe the effect of the variable dielectric constant on the problem of space-charge fields in insulators. First we elucidate the dependence of the electric polarization P on the voltage across the sample. Then we discuss Poisson's equation and the space-charge current relations. We here consider the infinitesimal-current case in which there is exact balance between diffusion and drift currents. In a forthcoming work we will discuss the finite-current situation, but for the present we treat the $J \approx 0$ limit for both the one- and two-carrier cases. The maximum intensity of the field will be at the electrodes. The boundary conditions at the electrodes depend on the two "insulator-electron-affinity-metal-work-function" potential differences (impd). We especially wish to show the influence that a variable K can have on the trend of the field.

A. Nature of Nonlinear Dielectric and Constitutive Relations

For most dielectrics, P increases in a linear fashion until the sample nears saturation. The dotted curve in Fig. 1 illustrates the usual dielectric behavior as exemplified by glass where the saturation occurs at such high fields that dielectric breakdown may take place. Aisenberg²⁶ reports that for high fields the nonferroelectric materials, aluminum oxide and tantalum oxide, exhibit a lowering of the dielectric constant.

Typical ferroelectrics have a much greater initial slope, a much smaller saturation field, and exhibit hysteresis characteristics which are discussed in the above-cited review articles. We are concerned with the application of a potential difference across an unpolarized sample. If the magnitude of the resulting field does not exceed the saturation field, the polarization curve is reversible. Note that in Fig. 1 we illustrate the nonlinear dielectric properties for a material like BaTiO_3 . For small fields this material displays a high dielectric constant (≈ 1000), while for higher fields (E much above the saturation field) it is much lower^{2,3} ($\approx 5-10$). Thus, the nonlinear insulator displays an initial slope greater than for the case of glass; this is maintained to a field E_1 where the polarization enters a transition region and begins to level off to its higher-field linear behavior which occurs for

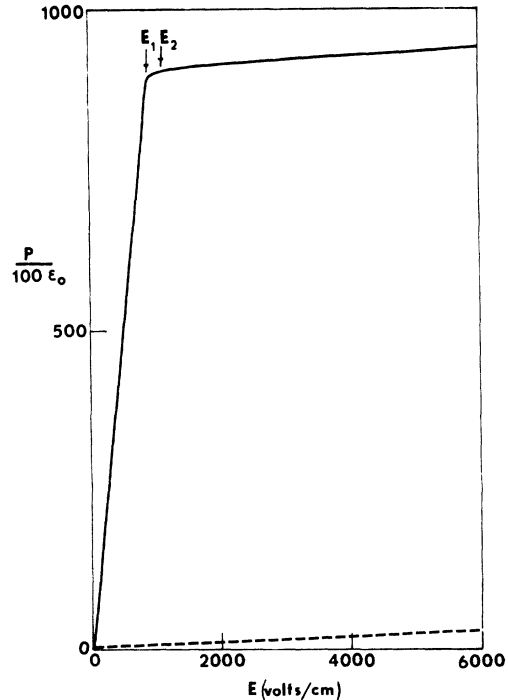


FIG. 1. Polarization as a function of E for a typical dielectric glass ($K=5$) and a typical ferroelectric (BaTiO_3) where $K=1000$. Note that for $E_2 > E > E_1$ the slope of the polarization falls to that of glass. In most texts the low-field region of $P(E)$ shows an "S" shaped bend in the initial rise from an unpolarized sample. This has been attributed to domain-wall motion. We assume a perfect single crystal and hence a linear P -vs- E curve in the low-field region.

fields greater than E_2 . In this region we show the slope to be approximately the same as glass.

The initial very strong response of the ferroelectric to the applied field has been interpreted as being due to opposite movement of the positive and negative ions in the unit cell,²⁷ and is an effect of lattice polarization. Below, we shall discuss the interplay of the nonlinear polarization and the internal electric field.

We are not treating a time-dependent case, and thus we emphasize that we describe a layered structure. That is, as a function of x , some layer may be highly polarized while a neighboring one may be unpolarized, so that if one region sustains a very high electric field, it may no longer be reversible, but that doesn't affect the field distribution we describe. What is essential is that a "virgin" sample is initially assumed. Thus, we consider herein the application of electrodes to such a sample.

At the boundary between the polarizable insulator and the metallic electrode the longitudinal component of the electric displacement D can have a discontinuity due to the buildup of a free-surface-

charge density in the dielectric. The D field is related to P and E_{int} , the internal electric field, by

$$D = \epsilon_0 E_{\text{int}} + P, \quad (1)$$

where ϵ_0 is the susceptibility of free space. Here we assumed the metal-insulator contact is over a large flat area thus leading to planar geometry and a dependence of our field variables on only the normal coordinate. By definition

$$P = (\epsilon - \epsilon_0)E_{\text{int}} = \epsilon_0(K - 1)E_{\text{int}}, \quad (2)$$

where ϵ is the dielectric's susceptibility and K is the dielectric constant; hence,

$$K = 1 + P/\epsilon_0 E_{\text{int}}. \quad (3)$$

As mentioned in the introduction to this section the high initial value of K is due to the movement of the ions in response to the electric field. Hence, as the dielectric becomes saturated and the lattice can no longer respond as strongly to increases in the external field, K must fall sharply to a low value.

Thus, increases in the applied voltage result in increases in the electric field with no extensive polarization changes.

B. Poisson's Equation for the Internal Electric Field

Having presented in Fig. 1 the constitutive relation between the polarization P and E_{int} , we now discuss Poisson's equation for a nonlinear dielectric. We assume that the surface dimensions of the insulating crystal are much larger than its thickness. The surfaces are in close contact with metal electrodes. At this point we mention our convention that the anode is taken to be at $x=0$ and the cathode at $x=L$. The resulting space charge transferred from the cathode and anode into the crystal gives rise to a field distribution which contributes to E_{int} . The field and space-charge distributions have been discussed in detail by many authors²²⁻²⁵; however, these authors have confined their treatments to the constant- K case. For the planar geometry we are considering

$$\frac{d}{dx} D = \epsilon_0 \frac{d}{dx} (K E_{\text{int}}) = \rho, \quad (4)$$

where ρ is the net free-charge density.

We shall consider two models for the space charge: (a) the one-carrier model with diffusion, (b) the two-carrier model with recombination centers. Throughout we treat the carrier mobility μ as a field-independent quantity. In the range of fields with which we are dealing, this is a very good approximation and the corrections derived by Dacy²⁸ and Lampert²⁹ do not apply. Expanding the derivative in Eq. (4), we write

$$\frac{dE_{\text{int}}}{dx} = \frac{1}{K} \left(-E_{\text{int}} \frac{dK}{dx} + \frac{\rho}{\epsilon_0} \right) = \left(1 + \frac{d \ln K}{d \ln |E_{\text{int}}|} \right)^{-1} \frac{\rho}{K \epsilon_0}. \quad (5)$$

Here we have used the chain rule and the fact that K is monotonically decreasing as the magnitude of E increases. This, of course, emphasizes our assumption that the polarization is reversible where the field is not too high. Then we can write the relationship

$$\left(\frac{E_{\text{int}}}{K} \frac{dK}{dx} \right) \left(\frac{dE_{\text{int}}}{dx} \right)^{-1} = \frac{E_{\text{int}}}{K} \frac{dK}{dE_{\text{int}}} = \frac{d \ln K}{d \ln |E_{\text{int}}|} < 0. \quad (6)$$

We are particularly interested in the "extra" term in Eq. (5) which arises from the variable dielectric constant. From Eq. (6) this term has the property

$$\text{sgn} \left(-\frac{E_{\text{int}}}{K} \frac{dK}{dx} \right) = \text{sgn} \left(\frac{dE_{\text{int}}}{dx} \right).$$

Also, $d \ln K / d \ln |E_{\text{int}}|$ is negative. For $E_1 < |E_{\text{int}}| < E_2$, the intermediate range, $|E_{\text{int}}|$ and K are almost inversely proportional; therefore, $d \ln K / d \ln |E_{\text{int}}|$ is slightly less than unity such that the factor in Eq. (5),

$$1 + \frac{d \ln K}{d \ln |E_{\text{int}}|} > 0. \quad (7)$$

Further, because of the monotonic constitutive relationship, if $dE_{\text{int}}/dx=0$, then $dK/dx=0$. This occurs only when ρ is zero. From the above, the first term in Eq. (5), $-(E_{\text{int}}/K)(dK/dx)$, can never be of opposite sign to the second term $\rho/K\epsilon_0$; thus, the first term acts as an enhancement to the effect of ρ on the trend of E_{int} .

Since the anode-insulator potential difference (i. e., the impd) is such that electrons face a potential barrier in passing from $x < 0$ to $x > 0$, E_{int} is positive at $x=0$; the electric field at $x=L$ may either be positive or negative. In the case of a semi-infinite insulator or one which is electroded on one face only, there is no *virtual cathode* (vik) and E_{int} does not change sign. For a thin insulator with two electrodes, there may or may not be a vik between $x=0$ and $x=L$. When the electrodes are similar materials so that the impd at $x=0$ and $x=L$ are not too different, we can have a vik within the insulator. It is this latter case, the thin sample one, which makes closest contact to Wright's treatment²⁵ of the $J \neq 0$ case where he shows the vik occurring nearer the cathode. However, when $J=0$, the vik, if it exists, may occur anywhere between 0 and L . When the impd is smaller at the cathode and larger at the anode, and $J \approx 0$, the vik occurs very close to the anode. For $J=0$ the vik occurs toward that electrode which has the smaller (electron) charge density (larger impd). For finite J the vik is never closer to the anode unless the

charge density is *substantially* smaller there. We discuss these cases below in Sec. IID. They have already been discussed in certain special cases by Skinner.²²

Now the trend of E_{int} with position is determined from Eq. (5). The sign of ρ determines whether E_{int} will increase or decrease as a function of x . The carrier density is fixed by the impd at the surface. If ρ is negative (electrons are the one carrier) and there is a vik, E falls from its positive value at the cathode through zero and then becomes negative deeper in the sample. From Eq. (5) we see that in a region where E is greater than E_1 , both dK/dx and ρ are negative so that dE_{int}/dx becomes larger in magnitude as we move away from the vik toward either surface. Thus, the larger values of the electric field are confined to the surface region. Recall that the electrodes are applied to an initially unpolarized "virgin" sample so that we are describing a layered electric structure. Let us now consider the form of the charge density in the above-mentioned models (a) and (b).

C. Charge Density and Electric Field in One-Carrier Model

For the one-carrier space-charge model with no traps [model (a)] in the case of electrons,

$$\rho(x) = -en(x) < 0. \quad (8)$$

Here e is the magnitude of electronic charge and n is the carrier density. Using the Einstein relation, $\mu kT = eD$, where D is the diffusion coefficient, the charge density is determined from the space-charge-limited current equation (transport equation),

$$J = e\mu n E_{int} + \mu kT \frac{dn}{dx}. \quad (9)$$

Thus,

$$n(x) = n_0 u(x, 0) + (J/\mu kT) \int_0^x dx' u(x, x'), \quad (10)$$

where

$$\begin{aligned} u(x, x') &= \exp\left[-(e/kT) \int_{x'}^x dx'' E_{int}(x'')\right] \\ &= \exp\{e[V(x) - V(x')]/kT\}; \end{aligned} \quad (11)$$

when J is quite small, it is clearly seen that $n(x)$ is given by a Boltzmann distribution and that $n(0) = n_0$ and $n(L)$ are given by the impd at the anode and cathode, respectively.

We may now integrate Eq. (6) to obtain $E_{int}(x)$ directly

$$E_{int}(x) = \left(\frac{K(0)E_{int}(0)}{K(x)} + \frac{1}{\epsilon_0 K(x)} \int_0^x \rho(x') dx' \right). \quad (12)$$

Rather than utilize the dielectric constant K , we have found it very helpful to discuss Poisson's equation and the position dependence of n and E in terms of a "dielectric parameter" K_p . The quantity in the denominator of Eq. (5) is [from Eq. (3)]

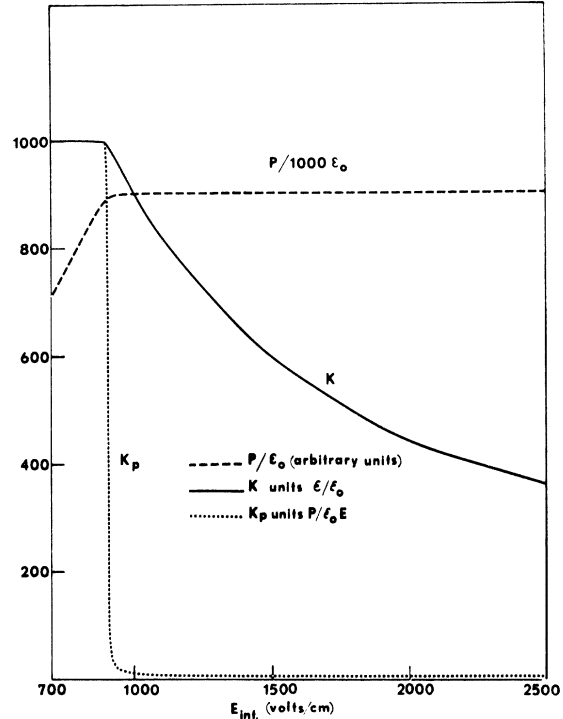


FIG. 2. Dielectric constant for a material like BaTiO_3 , $K = 1 + P/\epsilon_0 E_{int}$, and the dielectric parameter $K_p = 1 + (1/\epsilon_0) \times (dP/dE_{int})$ are shown as functions of E . For the convenience of the reader, the function P/ϵ_0 obtained in Fig. 1 is also shown.

$$K + E_{int} \frac{dK}{dE_{int}} = K + E_{int} \frac{d(P/\epsilon_0 E_{int})}{dE_{int}} = 1 + \frac{d(P/\epsilon_0)}{dE_{int}} \equiv K_p. \quad (13)$$

Then we can write Poisson's equation as

$$\frac{dE_{int}}{dx} = \frac{\rho(x)}{\epsilon_0 K_p(x)}. \quad (14)$$

Notice that if $K = \text{const}$, then $K_p = K$. However, P vs E_{int} can be linear (implying $K_p = \text{const}$) while $K \neq \text{const}$. This occurs if the extrapolated linear portion of the polarization curve does not go through the origin. Then,

$$K = K_p + [P_0/\epsilon_0 - (K_p - 1)E_0]E_{int}^{-1}, \quad (15)$$

where P_0 and E_0 are the values at the beginning of a linear region ($K_p = \text{const}$).

As already mentioned $K_p = K \approx 1000$ for $E < E_1$; also, the slope of P vs $\epsilon_0 E$, K_p , is about 5 for $E > E_2$. Thus, Eq. (2) and Fig. 1 lead to our chosen constitutive relation, the polarization-vs- E_{int} behavior shown in Figs. 2 and 3. Here P/ϵ_0 rises linearly from zero to the value 899.1 at $E_1 = 900$, quickly turns over to the value 899.5 at $E = 901$, continues the turnover to the value 901.3 at $E_2 = 1100$, and continues to rise linearly with a much reduced slope ($= 4$) for $E > E_2$. Note that the change

in K is stretched out over a very large electric field range. Using the values of P/ϵ_0 and its slope at E_1 and the high-field value of the slope, we fit P/ϵ_0 to a cube-root formula in terms of E . Then K and K_p follow from Eqs. (3) and (13), respectively.

One must then distinguish between K and K_p . K [see Eq. (3)] represents the total capacity of the material compared to that of the vacuum. K_p [see Eq. (13)], on the other hand, describes the ability of the material to allow further differential increments of P due to increments of E_{int} , i. e., the ability of the material to store *additional* charge. This quantity would be inversely related to the "spring constant" of the molecules of the dielectric, i. e., the strength of the ion couplings as discussed before Eq. (1) above. High values of K_p are associated with a very loose coupling while $K_p = 1$ implies an infinitely stiff one.

Examination of Eqs. (10)–(12) in the light of our introduction of K_p leads to a qualitative understanding of the behavior of $n(x)$ and $E_{int}(x)$. If $\rho(x)$ is negative (charge carriers are electrons only), it is clear that $E_{int}(x)$ tends toward negative values. In the region $0 < x < x_{vik}$, the electron density itself falls more than it would if K_p were not a function of E_{int} . This follows from the fact that dE_{int}/dx is proportional to n/K_p while dn/dx is proportional to nE . If $|E_{int}|$ falls below 900 V/cm, K_p rises sharply such that dE_{int}/dx falls in magnitude. This means the value of E_{int} falls more slowly which in turn keeps dn/dx high and drives n to lower values. If there is a vik, E_{int} changes sign and $n(x)$ has a minimum. Then for $x > x_{vik}$ as n begins to grow, the second term on the right-hand side in Eq. (12) dominates the first term. As E_{int} increases in magnitude, K_p shows its field dependence by falling off quickly; this in turn acts back on dE_{int}/dx to cause a further growth in E_{int} . Thus, the direct effect of $K_p(E)$ on E_{int} in this region is further enhanced by the indirect influence of K_p on the charge density.

D. Solution of Combined One-Carrier Transport and Poisson's Equations

In much of the dielectric, K_p takes on a constant value. In that case substitute Eq. (14) into Eq. (9), integrate, and obtain

$$\alpha(x) \equiv E^2(x) + \frac{2kT}{e} \frac{dE}{dx} = - \frac{2Jx}{\epsilon_0 \mu K_p} + \alpha_0, \tag{16}$$

where a subscript means the function evaluated at the corresponding value of x .

The mathematical treatment of the zero-current case is the limiting behavior for small current and thin sample. Under noninjection conditions we discuss two cases: (i) $\alpha_0 \geq 0$ which behavior joins smoothly to what we call the asymptotic boundary condition, $n_\infty = 0$, which from Eqs. (14) and (16) implies that $\alpha_0 = E_\infty^2$; (ii) $\alpha_0 < 0$ describes the "limited-region behavior" which occurs when the relative initial field derivative or charge density is high. For $J = 0$ we easily solve Eq. (16) by separation of variables:

$$E(x) = \alpha_0^{1/2} \left(\frac{\beta e^{\xi} + 1}{\beta e^{\xi} - 1} \right) = \frac{2kT}{e} \frac{d}{dx} \ln(\beta^{1/2} e^{\xi/2} - \beta^{-1/2} e^{-\xi/2})$$

$$= |\alpha_0|^{1/2} \times \begin{cases} \coth(\frac{1}{2}\xi + \frac{1}{2}\ln\beta), & \alpha_0 > 0 \\ \cot(\frac{1}{2}\xi + \gamma), & \alpha_0 < 0 \end{cases} \tag{17}$$

where

$$\xi = |\alpha_0|^{1/2} ex/kT,$$

$$\beta = \begin{cases} \frac{E_0 + \sqrt{\alpha_0}}{E_0 - \sqrt{\alpha_0}}, & \alpha_0 > 0 \\ e^{2i\gamma}, & \alpha_0 < 0 \end{cases}$$

$$\cos\gamma = E_0 \left[- \frac{2kT}{e} \left(\frac{dE}{dx} \right)_0 \right]^{-1/2},$$

$$\sin\gamma = (-\alpha_0)^{1/2} \left[- \frac{2kT}{e} \left(\frac{dE}{dx} \right)_0 \right]^{-1/2}.$$

We match the applied potential with these solutions:

$$0 > V_L = - \int_0^L E(x) dx = - \frac{2kT}{e} \times \begin{cases} \ln \left(\frac{\sin(\frac{1}{2}\xi_L + \gamma)}{\sin\gamma} \right), & \alpha_0 < 0 \\ \ln \left(\frac{\sinh(\frac{1}{2}\xi_L + \frac{1}{2}\ln\beta)}{\sinh(\frac{1}{2}\ln\beta)} \right), & \alpha_0 > 0. \end{cases} \tag{18}$$

In the special case $\alpha_0 = 0$, these expressions reduce to

$$E(x) = E_0(1 + eE_0x/2kT)^{-1},$$

$$V_L = (-2kT/e) \ln(1 + eE_0L/2kT). \tag{19}$$

For case (i) we see that both n and E are positive

monotonic decreasing functions of x . The electric field being positive, it points along the positive x axis so that there is a vik outside the material near the cathode.

For case (ii) we see that E is monotonic decreasing and n is always positive, but E can go negative.

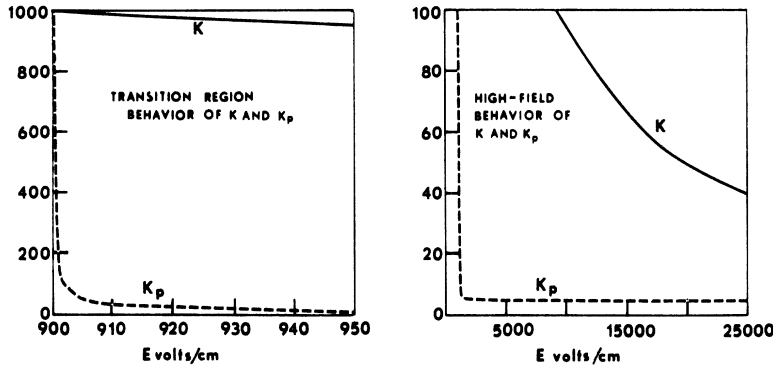


FIG. 3. K and K_p as functions of E_{int} in the transition regions $E_1 < E < E_2$ and in the high-field limit $E \gg E_2$. Note that even for $E = 25\,000$ V/cm, K has not yet reached its limiting value of 5.

When $E = 0$, $dn/dx = 0$ and n changes from a decreasing function to an increasing one. From Eq. (17), $E = 0$ when

$$x = x_{vik} = (\frac{1}{2} \pi - \gamma) 2kT/e |\alpha_0|^{1/2}, \quad \alpha_0 < 0. \quad (20)$$

This gives the position of the vik. Note that as

$|\alpha_0| \rightarrow 0$, $x_{vik} \rightarrow \infty$, so that in effect the vik is displaced outside the material as in case (i). Of course, γ and α_0 are limited by physical restrictions such as keeping E finite. We show in Figs. 4 and 5 $E(x)$ for $\alpha_0 < 0$ and $\alpha_0 > 0$, respectively. The analytical solutions are the same as we find by

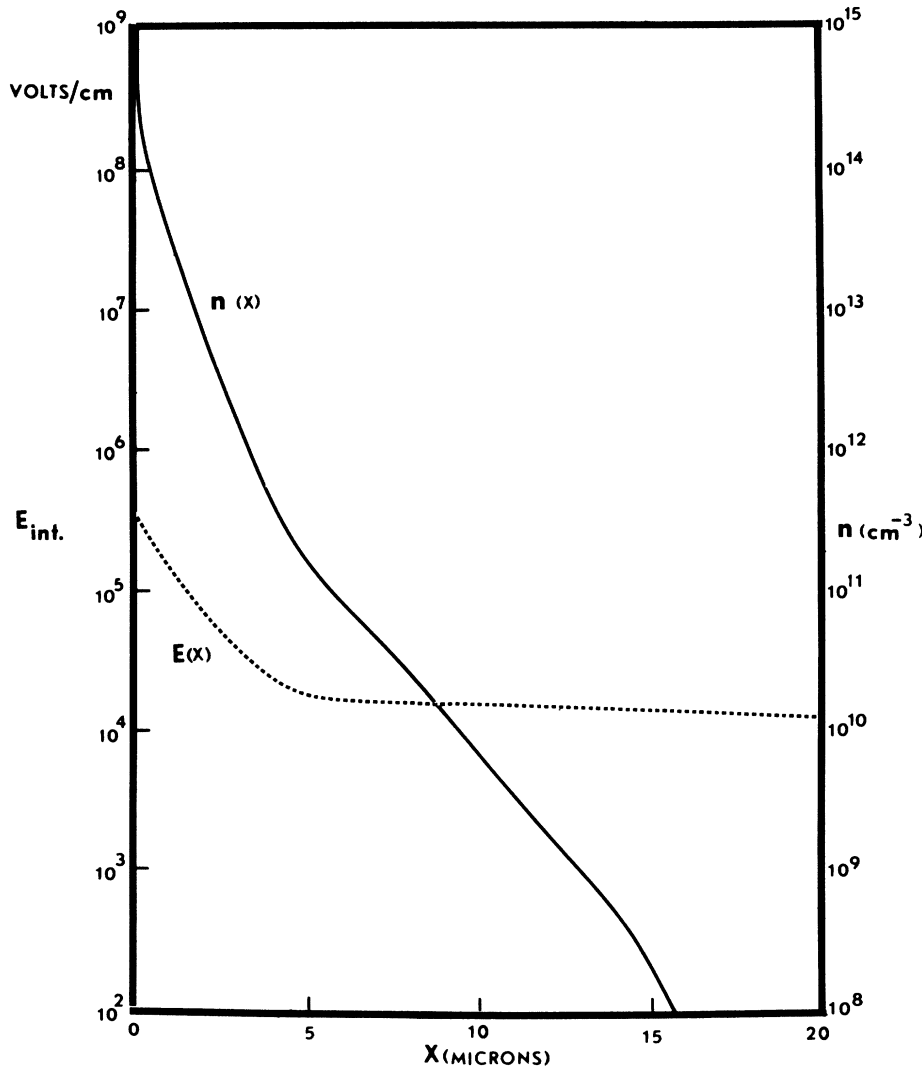


FIG. 4. E as a function of x for the constant- K case with $\alpha_0 > 0$. There is no vik and E falls to a constant limiting value.

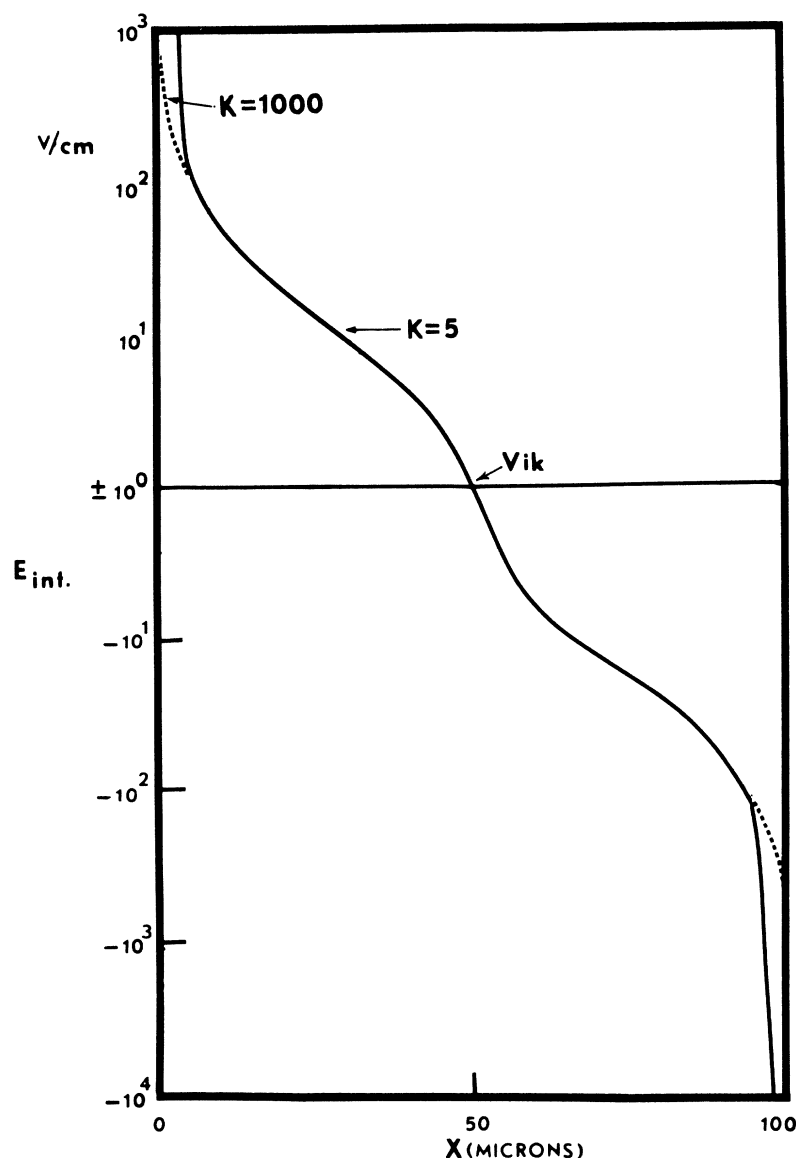


FIG. 5. E as a function of x in the constant- K case for $K=5$ and 1000. This is for $\alpha_0 < 0$, and the vik is at the center. The results are the same for either an analytical or a numerical solution.

using the numerical routines which we employ when K_p may be a variable.

The numerical solutions of the system of two equations [(9) and (14)] for the electric field, electric density, and voltage were obtained by a standard fourth-order Runge-Kutta technique. The programs were executed on a CDC-6500 computer, the speed of which allowed for a very fine grid of points (20 Å per point) which is necessary since the calculated functions are very sensitive to position near the surface. We present the results of these calculations in Fig. 4 through Fig. 11. For the purposes of this $J=0$ calculation, T was taken at 300 °K, while μ was set for BaTiO₃ at 0.1 cm²/V sec.²³

Figure 5 shows $E(x)$ for $K_p=1000$ and 5. $n(0)$ is

the same for both cases, and to have a vik at the center, it is required to have a larger electric field at the surface. Of course, if $E^2(0)$ is so large with respect to $(2kT/e)[dE(0)/dx]$, which in turn is determined by $n(0)$, that $\alpha_0 > 0$, then there will be no vik as was shown in Fig. 4 and discussed above. Figures 6 and 7 show the $n(x)$ and $V(x)$ (charge density and voltage) in the cases described in Fig. 5.

In Figs. 8 and 9 we consider the near-surface region for a material with K_p small. $E(0)$ and $n(0)$ are same as for Fig. 5. In this case, K_p is small only in the region $|E| < |E_1|$. As soon as E falls below 900 V/cm, dE/dx becomes reduced by a factor of 200 since in the very narrow region where K_p varies $n(x)$ is essentially constant. Thus, for a variable K_p , in the region where K_p has its high

values, we have a situation where E remains constant and then $n(x)$ falls toward zero, such that there is no vik. However, we do not believe that the above behavior is appropriate here, i. e., that the vik disappears for the variable K_p case. What we should do is compare the large K_p case with the variable K_p case. Let us assume a vik exists in the bulk of the material (see Fig. 5). The field rises in value toward 900 V/cm as we approach the surface from within. Then E will rise above the value it would have if K_p kept its large value (see Fig. 10). Also, we see from Fig. 11 that n rises to ≈ 70 times its $K_p = \text{const} = 1000$ value. Thus, we are led to the result that the electron density near the surface is much larger for the small K_p case. This seems reasonable to us when we consider that the

electron-affinity potential should depend on the image field seen by electrons approaching the boundary from the metal. The image field in turn depends on the inverse of the dielectric parameter.

Note that when one is dealing with linear-response theory, K_p^{-1} is found to be the inverse dielectric constant. This can be understood from the fact that the space charge in the surface region of the insulator sets up a field which is shielded by the polarization charge. When this field becomes large enough to change K_p , the shielding of the attractive mirror charge drops and further charge becomes attracted into the surface region from the electrode.

Let the reader notice that the figures showing the vik in the center of the sample can be used to exhibit the case when the vik is (far) off-center. This

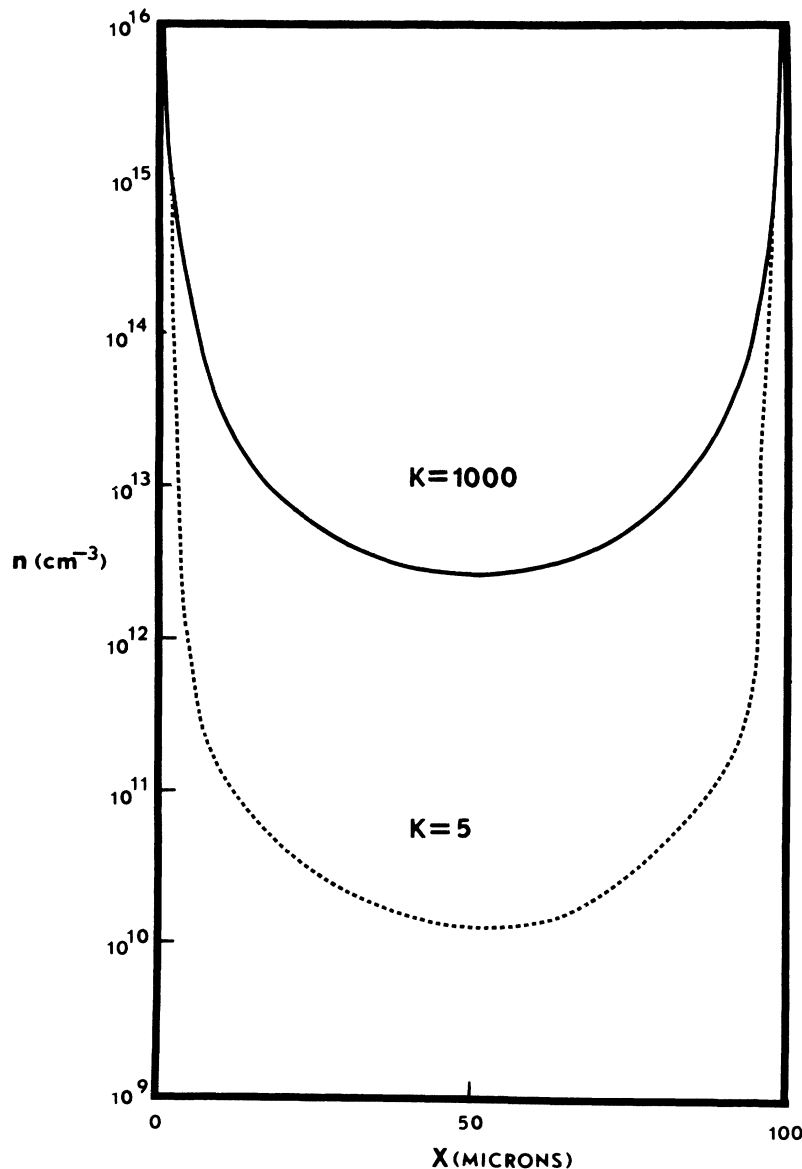


FIG. 6. $n(x)$ for the constant values of K , 5 and 1000.

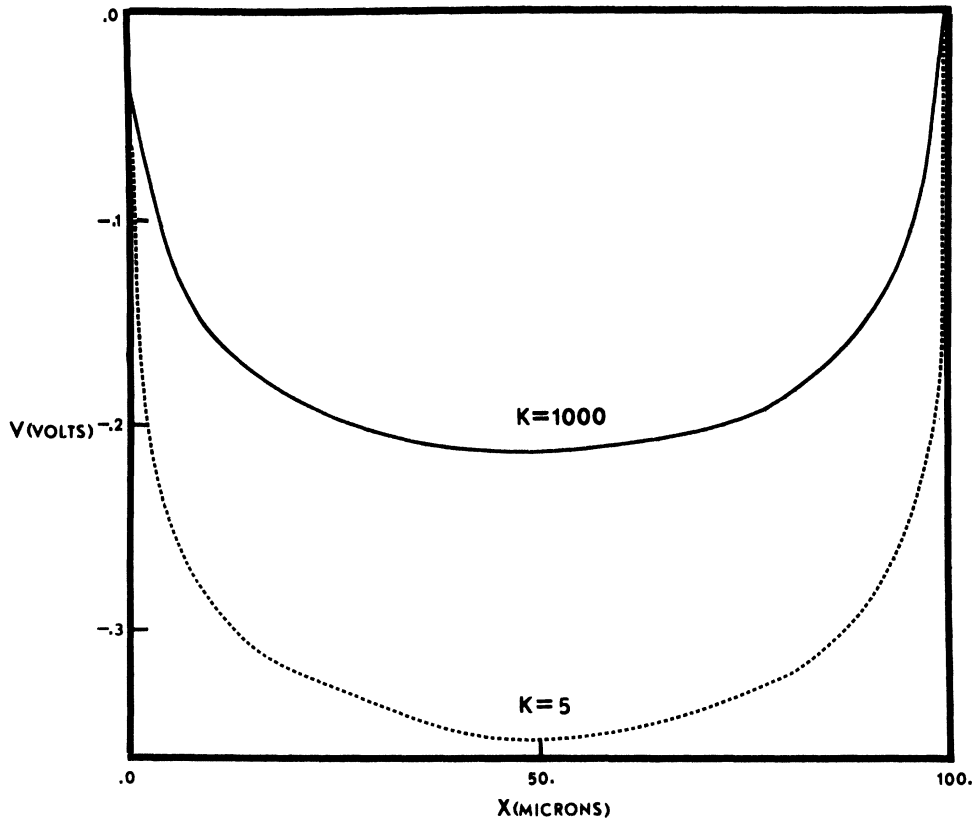


FIG. 7. $V(x)$ for the constant values of K , 5 and 1000.

is done by cutting off the curve on either side, thus destroying the center of symmetry. Note from Figs. 5 and 6 that n and $|E|$ at the surface nearer to the vii have much smaller values than at the other surface.

E. Two-Carrier Model of Electric Field and Charge Density

We next briefly consider the two-carrier formulation [model (b)]. Since BaTiO_3 has extremely low carrier mobility (associated with its high resistivity), we may consider $J=0$ as a reasonable first approximation to the low currents normally observed. In this $J=0$ limit, the electrons and holes decouple, and we can deal with the problem taking into account carrier diffusion as well as carrier drift. An appropriate charge density $\rho(x)$ may be given by

$$\rho/e = p - n + P_R - P_{R_0}, \quad (21)$$

where n is the electron density, p the hole density, P_R the density of holes in recombination centers, or, equivalently, the density of electron traps, and P_{R_0} the equilibrium value of P_R when dealing with an isolated insulator, i. e., one without electrodes and which is not in the presence of an applied field. The space-charge equation appropriate to two-carrier flow in the zero-current limit is

$$\frac{J}{e} = \mu_n \left(nE + \frac{kT}{e} \frac{dn}{dx} \right) + \mu_p \left(-pE - \frac{kT}{e} \frac{dp}{dx} \right). \quad (22)$$

The first term on the right-hand side gives the drift and diffusion contribution of the electrons, while the second term on the right-hand side gives these contributions for the holes. The respective carrier mobilities are μ_n and μ_p . It should be noted that the Einstein relations for the diffusion coefficient have been employed; i. e., $\mu_n kT = eD_n$ and $\mu_p kT = eD_p$. In our special case of $J=0$ (which is always accompanied by $J_n = J_p = 0$), we can write down the solutions

$$n(x) = n(0)u(x, 0), \quad (23)$$

$$p(x) = p(0)n(0)/n(x), \quad (24)$$

$$P_R = N_R / \left(1 + \frac{\langle v\sigma_n \rangle n}{\langle v\sigma_p \rangle p} \right), \quad (25)$$

where $u(x, 0)$ and $n(0)$ [and $p(0)$ by analogy] are given above in Sec. IIC on the one-carrier model, and where N_R is the total trap density, v the drift velocity, σ_n the cross section for electron capture, and σ_p the cross section for hole capture. We assume $\langle v\sigma_n \rangle$ and $\langle v\sigma_p \rangle$ are independent of the electric field.³⁰

Let us now examine Poisson's equation in the case

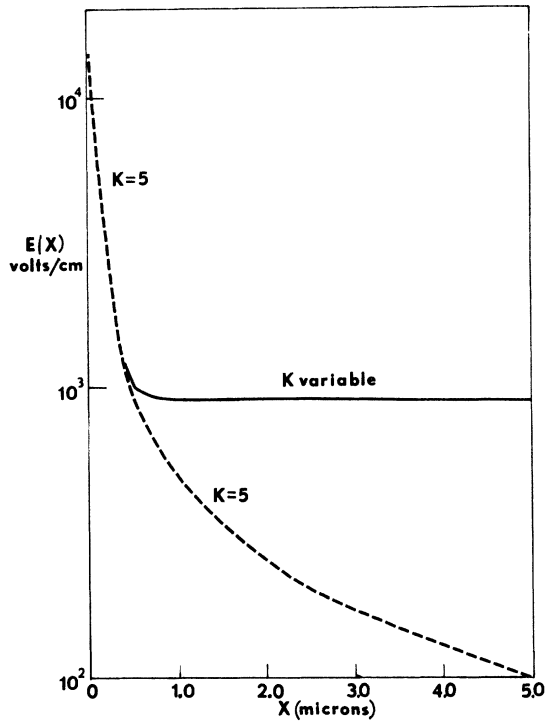


FIG. 8. $E(x)$ in the surface region. Note that in the variable- K_p case, when E falls below 900 V/cm, E becomes a constant. In effect, the vik is removed.

that the charge density is given by Eq. (21). This will yield some idea of the electric field structure. We assume $\rho(x=0) < 0$. Thus, the field at the surface $x=0$ is rather similar to that of the one-carrier case; that is, the field is positive at $x=0$, and falls to zero at $x=x_{vik}$ and increases negatively as $x \rightarrow L$. The charge density which is negative at $x=0$ cannot go to zero to the left of x_{vik} ; otherwise, it would imply that E_{int} has a turnover and no virtual cathode could exist. If there is a vik within the insulator, then to the right of x_{vik} , n increases while ρ and P_R decrease. This may be seen by examining Eq. (11) and Eqs. (23)–(25). Therefore, in this region ρ grows more negative [so long as $\rho(x_{vik}) < 0$] and cannot reach zero. We are forced to assume then that ρ can equal zero only at $x=x_{vik}$, and we conclude that the fields are qualitatively similar to the one-carrier case. Again the sharpest variations of E_{int} are in the near-surface region where the variable K enhances the fall of E_{int} . The introduction of two carriers tends to diminish the magnitude of the net charge density in the interior (nonsurface) regions and serves to make the variation of E_{int} with x more mild there.

We may mention that the high-current formalism employed by Waxman and Lampert³⁰ results in a self-consistent change in the sign of the charge density. This leads to a turnover of the negative field

and a large field in the interior as well as at the surfaces. We will discuss this more quantitatively in a forthcoming paper.

Our analysis is in broad agreement with reported measurements³¹; however, a more detailed theoretical, as well as experimental, study is necessary before a quantitative evaluation can be made. There are investigations presently underway.

III. DISCUSSION OF OUR MODEL AND ITS APPLICATION TO ANOMALOUS RADIATION SENSITIVITY OF BaTiO_3

We have shown that in a thin ferroelectric sample the electric field, the charge-density distribution, and the impd have a very sensitive interrelationship to each other. This follows from the high polarizability at lower fields, but low polarizability at higher fields. This reflects itself in the sharp change in the dielectric parameter which in turn has a strong effect on the impd and, subsequently, the charge density at the surface. Now at the dielectric-electrode interface the charge density and electric field can range from very small to very large values. In a ferroelectric these equilibrium configurations are very delicate and are subject to upset from perturbations such as electromagnetic or acoustic radiation.

In the light of the results of our theoretical considerations let us consider the case of the radiation

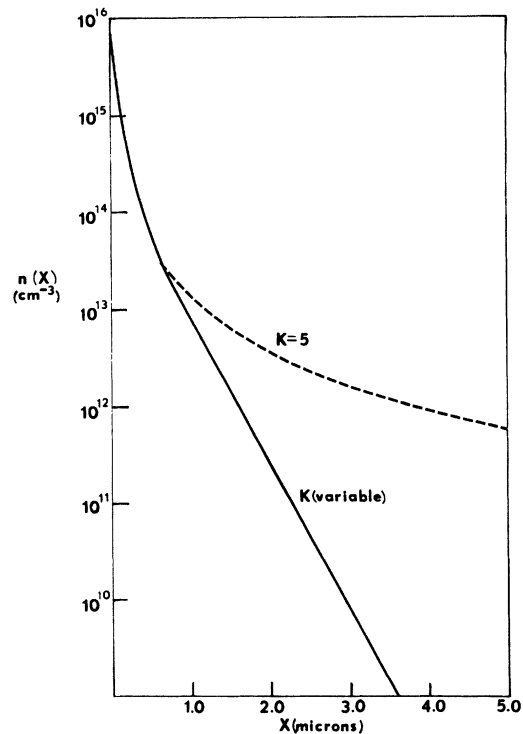


FIG. 9. $n(x)$ in the near-surface region with the same boundary conditions as in Fig. 8. When $E(x)$ falls below 900 V/cm, $n(x)$ begins to fall precipitously toward zero.

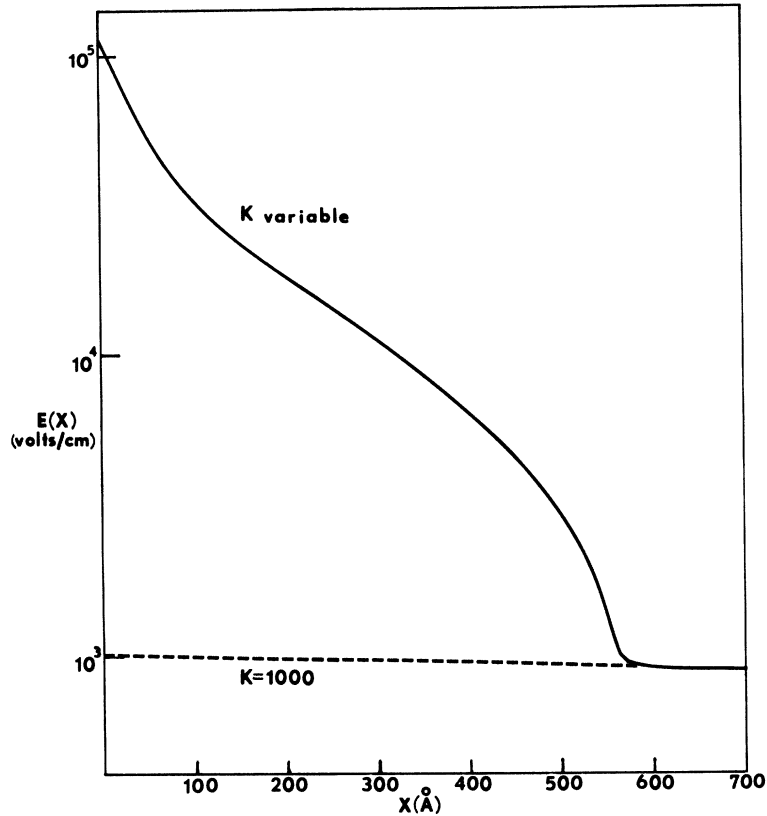


FIG. 10. $E(x)$ in the surface region if $n(0)$ is allowed to increase due to lowering of the K_p and increase of effect of mirror charge. For convenience the $K_p=1000$ case is also shown.

sensitivity of BaTiO_3 .¹² In this experiment Lefkowitz found that an emf was instantaneously generated when the sample was impinged upon by ionizing radiation which could only penetrate a very shallow region of the crystal.

This exhibited itself by a voltage pulse of one polarity immediately followed by one of equal magnitude and opposite polarity. Furthermore, the piezoelectric response of the irradiated region of the sample was destroyed. As the sample was repeatedly bombarded with radiation, the piezoelectric response to ambient noise gradually returned. These anomalous effects must be attributed to modifications of the field and charge distribution at the surface by the ionizing radiation.

Lefkowitz originally discussed these phenomena by assuming that the surface layers act like charged capacitors with capacities different from that of the bulk, and that these surface capacitors are shorted out by the electron-hole pairs produced in the surface region by the incident radiation. We would like to discuss his ideas in terms of our model constructed in Sec. II. The capacitance of a ferroelectric material is proportional to the dielectric constant; when the fields near the surface are very high, the polarizability falls as does the capacity to store more charge in the surface layer. In Sec. II we described an equilibrium situa-

tion in which the charge distribution has been allowed to reach a steady state and is smoothly behaved as a function of x and E_{int} . If, however, some disturbance (such as electromagnetic radiation impinging on the surface and creating numerous electron-hole pairs³²) introduces a nonequilibrium into the charge distribution, then the electric field will cause a redistribution of the extraneous charge. It was shown in Sec. IID that adding negative charge makes the field fall off more quickly as a function of x . The created holes congregate at the vik if there is one within the sample; otherwise, they drift toward the cathode. The probe electrode will in general have a different impd than the electrode on the inactive surface. A smaller impd at the active surface gives rise to larger electric fields and electron densities than on the other surface, and vice versa.

In Lefkowitz's experiment¹² we assume that the incident x rays produced electron-hole pairs very close to the surface. We have illustrated the drift of the electron and hole components in the cases where there is a vik within the sample (Fig. 12) and for no vik (Fig. 13). If E decreases in magnitude from the active surface toward the interior, electron ejection occurs. On the other hand, if E increases in magnitude from the active surface toward the interior of the sample, the holes migrate

toward the surface, thus attracting electrons from the probe; i. e., electrons are injected. For the rare situation where the vik is very near the surface, there is equal probability for electron-hole pairs to be produced closer to or further from the surface than the vik, thereby resulting in electron ejection or injection, respectively.

Recall that for the low K , and high E in the near-surface region most of the energy is stored in the field. If the radiation has impinged on a high-field region, the electric field will accelerate the electron component toward this surface. This takes energy from the field structure; thus, its magnitude must decrease. Hence, it cannot sustain the large associated equilibrium electron charge density. The electrons are expelled into the probe. This produces the large observed emf pulse. Because the impd was unaffected by the radiation, thereafter electrons rush back into the dielectric giving rise to the pulse of opposite polarity. This we describe as ejection followed by injection.

It was further observed in this experiment that

the leading pulses recorded by the small probe at one part of the surface were often of opposite polarity to leading pulses measured at another near-surface location. This may be explained as follows. If the radiation falls upon a low-field region, the holes will collect at this surface (see Fig. 13). These will attract electrons into the sample from the probe, giving rise to an initial emf pulse opposite in polarity to the electron-ejection case. The electrode now lacks some of its equilibrium electrons. Some of the metals' surface-electric-field energy has been used to accelerate the electrons into the insulator. Subsequently, additional electrons are injected from the metal because the diminished magnitude of the electric field on the electrode surface cannot support the former equilibrium electron density. Nonequilibrium occurs in the dielectric, and again the impd condition at this surface causes electrons subsequently to be ejected from the sample to replace electrons in the electrode. This condition is injection followed by ejection and is of opposite polarity to the

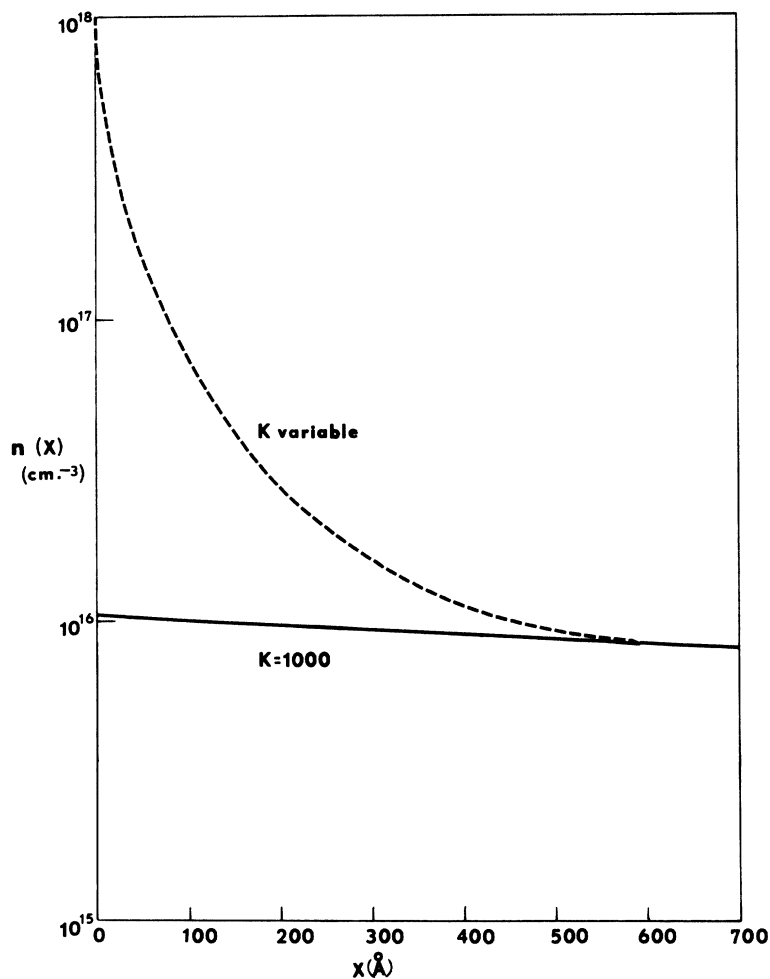


FIG. 11. $n(x)$ in the surface region for the situation described in Fig. 10.

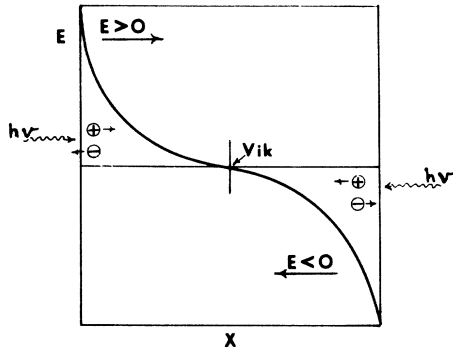


FIG. 12. When there is a vik within the sample, the holes flow toward the interior and the electrons flow toward the interface where they are accelerated by the high electric fields and are subsequently ejected into the electrode probe.

case described above.

After the sample has initially reacted to the x-ray radiation with an emf pulse pair, it is still in nonequilibrium. Therefore, the piezoelectric effect which depends on the electromechanical response of the ferroelectric in a given equilibrium situation would be destroyed. Lefkowitz did find, however, that if the sample is repeatedly bombarded at the rate of 50 x-ray bursts per sec, the piezoelectric response to the ambient sound gradually returns. We assume that the sample came to a new equilibrium under this regular irradiation pattern.

Note that the emf pluses were only observed when the electrode was quite small ($\approx 0.2 \text{ mm}^2$) and made an intimate bond to the surface of the sample. This too may be explained within our model. Since the probe pressed very tightly against the ferroelectric, the resulting strains in the BaTiO_3 affected its piezoelectric characteristics in such a way that the impd of the intimately bonded electrode-insulator pair was modified. Equally important are the surface impurities which affect the electron affinity. Therefore, the ferroelectric had in one region of the surface a higher impd than the electrode of the same material at the far side of the sample, while in an adjacent area the sample had a lower impd. If, however, the electrode probe area was too large, then the random nature of the distribution of relatively high- and low-impd regions (on the surface near the probe with respect to the opposite side of the sample) was such that both types would be included in a single measurement, and no net pulse could be observed.

Two other observations made in this experiment also may be mentioned briefly. It was noted that the voltage pulses were observed above the Curie point and showed no systematic thickness dependence. These observations, too, are consistent with the ferroelectric-surface-layer formulation.

That the pulses are observed above the Curie point indicates the existence of a tetragonal strain in the near-surface region at elevated temperatures. This is in agreement with Chynoweth's⁷ results for the pyroelectric effect, as well as with English's^{16,17} electron-mirror micrographs of the ferroelectric surface. The lack of thickness dependence in the voltage pulses shows that the effect is essentially limited to the surface regions.

It is of interest to note that there have been several unsuccessful attempts to measure these surface layers in which ionizing radiation was used. M. E. Drougard at IBM in an extremely careful and elegant x-ray measurement could find no evidence of a surface layer in a single crystal of BaTiO_3 .³³ Kay and Lefkowitz, using x rays, sought evidence for these layers in single crystals of BaTiO_3 near the Curie point, but could find no evidence for them.³⁴ Electron transmission photographs of thin single crystals of BaTiO_3 also failed to produce evidence for the layer.³⁵ On the basis of our above discussion it is to be expected that such experiments would not be successful in yielding evidence for a surface region. Indeed the probing x rays themselves break down the surface region and strongly modify the space-charge distribution. In contrast observations by optical methods should always be possible. Since the low K implies a shift of the soft mode to higher frequencies, evidence for this shift should be found in IR data. Such evidence was found and is discussed by Lefkowitz.³⁶

It is also useful to consider the implications of these surface fields once produced since they could be a source of serious difficulties in the use of dielectrics (i. e., for measurements of the Fermi surface by contact-potential methods or in application as capacitor materials). Under normal circumstances capacitors are inert devices with relative impd's distributed randomly over the surface. However, there is a small statistical probability

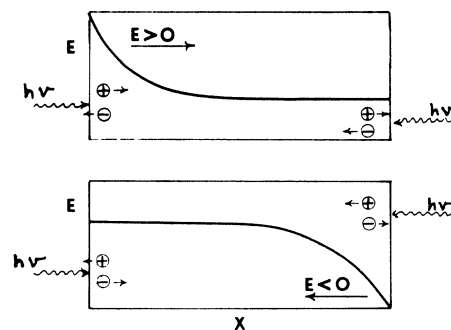


FIG. 13. When there is no vik in the sample, the holes pile up near the surface where the field strength is maximum. If the radiation impinges on that face of the sample, electrons will be attracted from the probe.

that this surface randomness does not occur; then a capacitor or a ferroelectric transducer could act as a random energy source. The occurrence of a large area over which the relative impd is uniform would be less likely in a ceramic than in an idealized single crystal. Even so such anomalous energy discharges have occurred, and if these particular dielectrics had been components in complex equipment systems, then the reliability of those systems would have been reduced.¹²

IV. SUMMARY

We have calculated the electric field distribution for a thin insulator for both linear and a model nonlinear polarization. The enhancement effects in the latter case has been delineated, and their implications have been discussed.

Many experiments have shown that a layer of low-dielectric-constant material can exist under certain conditions at the surface of ferroelectrics. This near-surface region is due to the high fields caused by the space charge within it. We have shown that such behavior at the surface can be explained by the mutual interplay of the nonlinear bulk dielectric constant and the large space-charge fields close to the surface. No special properties need be invoked to explain such behavior.

ACKNOWLEDGMENTS

We would like to thank Professor M. Caspari, Dr. M. Lampert, Dr. G. Vineyard, and Dr. F. Stern for their many helpful discussions, and S. Collins for his preliminary work on the material presented here.

¹W. Känzig, *Phys. Rev.* **98**, 549 (1955).

²F. Jona and G. Shirane, *Ferroelectric Crystals* (Pergamon, New York, 1962).

³W. Merz, *Progress in Dielectrics* (Academic, New York, 1962), Vol. 4.

⁴E. Fatuzzo and W. Merz, *Ferroelectricity* (North-Holland, Amsterdam, 1967).

⁵F. S. Galasso, *Structure, Properties and Preparation of Perovskite Compounds* (Pergamon, New York, 1969), p. 82.

⁶M. Anlicker, H. R. Brugger, and W. Känzig, *Helv. Phys. Acta* **27**, 99 (1954).

⁷A. G. Chynoweth, *Phys. Rev.* **102**, 705 (1956).

⁸S. Triebwasser, *Phys. Rev.* **118**, 100 (1960).

⁹J. R. Anderson, G. W. Brady, W. J. Merz, J. P. Remeika, *J. Appl. Phys.* **26**, 1387 (1955).

¹⁰V. Janovec, *Czech. J. Phys.* **9**, 468 (1959).

¹¹W. R. Bussem, E. C. Subbarao, *Naturwiss.* **44**, 509 (1957).

¹²I. Lefkowitz, *Nature* **198**, 657 (1963).

¹³I. Lefkowitz, *J. Phys. Chem. Solids* **10**, 169 (1959).

¹⁴I. Lefkowitz, K. Kramer, and P. Kroeger, Frankford Arsenal Report No. R-1779, 1964 (unpublished).

¹⁵V. A. J. Van Lint and M. E. Wyatt, General Atomic Report No. Ga-7777, 1968 (unpublished).

¹⁶R. L. English, *J. Appl. Phys.* **39**, 128 (1968).

¹⁷R. L. English, *J. Appl. Phys.* **39**, 3231 (1968).

¹⁸M. E. Drougard and R. Landauer, *J. Appl. Phys.* **30**, 1663 (1959).

¹⁹W. Merz, *J. Appl. Phys.* **27**, 938 (1956).

²⁰H. Schlosser and M. E. Drougard, *J. Appl. Phys.* **32**, 1227 (1961).

²¹G. Rupprecht (private communication), based on an extension of previous work.

²²S. M. Skinner, *J. Appl. Phys.* **26**, 496 (1955).

²³R. H. Tredgold, *Space Charge Conduction in Solids* (Elsevier, London, 1966).

²⁴M. Lampert and F. Edelman, *J. Appl. Phys.* **35**, 2971 (1964). See Ref. 3 of this paper for a review of previous solutions to this problem.

²⁵G. T. Wright, *Solid State Electron.* **2**, 165 (1961).

²⁶S. Aisenberg, *Bull. Am. Phys. Soc.* **12**, 984 (1967).

²⁷J. C. Slater, *Quantum Theory of Matter* (Addison-Wesley, Reading, Mass., 1967), Vol. III.

²⁸G. C. Dacey, *Phys. Rev.* **90**, 759 (1953).

²⁹M. A. Lampert, *J. Appl. Phys.* **29**, 1082 (1958).

³⁰A. Waxman and M. Lampert, *Phys. Rev. B* **1**, 2735 (1970).

³¹H. Motegi and S. Hoshino, *J. Phys. Soc. Japan* **29**, 524 (1970).

³²That a copious quantity of electron-hole pairs is needed for the breakdown effect to occur may be shown by the fact that there was a threshold intensity at which the voltage pulses were not observed.

³³M. E. Drougard (private communication).

³⁴M. Kay and I. Lefkowitz (private communication).

³⁵M. Tanaka and G. Honjo, *J. Phys. Soc. Japan* **19**, 954 (1964).

³⁶I. Lefkowitz, *Proc. Phys. Soc. (London)* **80**, 868 (1962).